medRxiv preprint doi: https://doi.org/10.1101/2023.07.24.23293124; this version posted July 27, 2023. The copyright holder for this preprint (which was not certified by peer review) is the author/funder, who has granted medRxiv a license to display the preprint in perpetuity. It is made available under a CC-BY-NC-ND 4.0 International license .

Systemic hypoxemia catalyzes cerebral oxidative-nitrosative stress during extreme apnea in humans: implications for cerebral bioenergetic function

Damian M. Bailey[1*], Anthony R. Bain[2*], Ryan L. Hoiland[3,4*], Otto F. Barak[5,6], Ivan Drvis[7], Benjamin S. Stacey[1], Angelo Iannetelli[1], Gareth W. Davison[8], Rasmus H. Dahl[9], Ronan M.G. Berg[1,10], David B. MacLeod[11], Zeljko Dujic[5*] and Philip N. Ainslie[1,12*]

[1]Neurovascular Research Laboratory, Faculty of Life Sciences and Education, University of South Wales, Glamorgan, UK; [2]Faculty of Human Kinetics, University of Windsor, Windsor, ON, Canada; [3]Department of Anaesthesiology, Pharmacology and Therapeutics, Vancouver General Hospital, West 12th Avenue, University of British Columbia, Vancouver, BC, Canada; [4]Department of Cellular and Physiological Sciences, Faculty of Medicine, University of British Columbia, 2350 Health Sciences Mall, Vancouver, BC, Canada; [5]School of Medicine, University of Split, Split, Croatia; [6]Faculty of Medicine, University of Novi Sad, Serbia; [7]School of Kinesiology, University of Zagreb, Zagreb, Croatia; [8]Sport and Exercise Science Research Institute, Ulster University Belfast, UK; [9]Department of Radiology, University Hospital Rigshospitalet, Copenhagen, Denmark; [10]Department of Biomedical Sciences, University of Copenhagen, Denmark; [11]Department of Anesthesiology, Duke University Medical Center, Durham, NC, USA and [12]Center for Heart Lung and Vascular Health, University of British Columbia, Kelowna, British Columbia, Canada

Running title: Redox-regulation of neurovascular complex function
Keywords: oxygen, carbon dioxide, free radicals, nitric oxide, cerebral bioenergetic function

*contributed equally

Corresponding author
Professor Damian Miles Bailey PhD FRSC FACSM FPVRI FTPS
Royal Society Wolfson Research Fellow
Director of the Neurovascular Research Laboratory
Alfred Russel Wallace Building
Faculty of Life Sciences and Education
University of South Wales
UK CF37 4AT

Telephone number: +44-1443-482296
Fax number: +44-1443-482285
*e*mail: damian.bailey@southwales.ac.uk
Webpage: http://staff.southwales.ac.uk/users/2240-dbailey1
Twitter: @USW_Oxygen and @DamianMBaileyEP
Orcid: https://orcid.org/0000-0003-0498-7095

NOTE: This preprint reports new research that has not been certified by peer review and should not be used to guide clinical practice.

medRxiv preprint doi: https://doi.org/10.1101/2023.07.24.23293124; this version posted July 27, 2023. The copyright holder for this preprint
(which was not certified by peer review) is the author/funder, who has granted medRxiv a license to display the preprint in perpetuity.
It is made available under a CC-BY-NC-ND 4.0 International license .

ABSTRACT

BACKGROUND: Voluntary asphyxia induced by apnea in competitive breath hold (BH) divers affords a unique opportunity to examine integrated mechanisms underlying the preservation of cerebral bioenergetic function. This study examined to what extent physiological extremes of oxygen (O_2) demand and carbon dioxide (CO_2) production impact redox homeostasis and corresponding red blood cell (RBC)-mediated cerebral vasodilation.

METHODS: Ten ultra-elite apneists (6 men, 4 women) aged 33 ± 9 (mean ± SD) years old performed two maximal dry apneas preceded by, [1] normoxic normoventilation resulting in severe hypoxemic hypercapnia apnea (HHA) and [2] hyperoxic hyperventilation designed to prevent hypoxemia resulting in isolated hypercapnic apnea (IHA). Transcerebral exchange kinetics of ascorbate radicals ($A^{\cdot-}$, electron paramagnetic resonance spectroscopy), lipid hydroperoxides (LOOH, spectrophotometry) and nitric oxide metabolites (NO, tri-iodide reductive chemiluminescence) were calculated as the product of global cerebral blood flow (gCBF, duplex ultrasound) and radial arterial (a) to internal jugular venous (v) concentration gradients determined at eupnea and after apnea.

RESULTS: Apnea duration increased from 306 ± 62 s during HHA to 959 ± 201 s during IHA (P = <0.001), resulting in individual nadirs of 29 mmHg and 40 % for PaO_2 and SaO_2 respectively in HHA and $PaCO_2$ peak of 68 mmHg in IHA. Apnea resulted in a more pronounced elevation in the net cerebral output (v>a) of $A^{\cdot-}$ and LOOH in HHA (P = <0.05 vs. IHA). This coincided with a lower apnea-induced increase in gCBF (P = <0.001 vs. IHA) and related suppression in plasma nitrite (NO_2^-) uptake (a>v) (P = < 0.05 vs. IHA), implying reduced consumption and delivery of NO consistent with elevated cerebral oxidative-nitrosative stress (OXNOS). While apnea-induced gradients consistently reflected plasma NO_2^- consumption (a>v) and RBC iron

medRxiv preprint doi: https://doi.org/10.1101/2023.07.24.23293124; this version posted July 27, 2023. The copyright holder for this preprint
(which was not certified by peer review) is the author/funder, who has granted medRxiv a license to display the preprint in perpetuity.
It is made available under a CC-BY-NC-ND 4.0 International license .

nitrosylhemoglobin formation (v>a), we failed to observe equidirectional gradients consistent with *S*-nitrosohemoglobin consumption and plasma *S*-nitrosothiol delivery.

CONCLUSIONS: These findings highlight a key catalytic role for hypoxemia in cerebral OXNOS with NO_2^- reduction the more likely mechanism underlying endocrine NO vasoregulation with the capacity to transduce physiological O_2-CO_2 gradients into graded vasodilation.

medRxiv preprint doi: https://doi.org/10.1101/2023.07.24.23293124; this version posted July 27, 2023. The copyright holder for this preprint (which was not certified by peer review) is the author/funder, who has granted medRxiv a license to display the preprint in perpetuity. It is made available under a CC-BY-NC-ND 4.0 International license .

INTRODUCTION

The neurovascular complex (NVC) is a recent concept that highlights the functional interaction between the multi-hetero-cellular structure comprizing the neurovascular unit (NVU) and the systemic vasculature[1]. Precisely how the NVC integrates, coordinates and processes molecular signals that collectively maintain cerebral blood flow (CBF) and structural integrity of the blood–brain barrier (BBB) remains to be fully understood, although emergent evidence suggests a key role for redox-regulation[2].

In support, a neuroprotective hormetic role has emerged for the physiological formation of free radicals and associated reactive oxygen/nitrogen species (ROS/RNS) that enable the sensing and subsequent clearance/delivery of the respiratory gases carbon dioxide (CO_2) and oxygen (O_2) to which the human brain has evolved exquisite sensitivity. In contrast, when excessive and sustained, free radical formation can result in structural destabilization and vascular impairment of the NVU subsequent to oxidative inactivation of vascular nitric oxide (NO), collectively termed oxidative-nitrosative stress (OXNOS)[3, 4].

However, to what extent O_2 and CO_2 tensions independently modulate NVC function including the potentially differential impact on the redox-regulation of nitrite (NO_2^-) and *S*-nitrosohemoglobin (SNO-Hb) bioactivity, the principal competing mechanisms underlying endocrine NO vasoregulation[5], remains to be established. Prolonged apnea performed by ultra-elite breath-hold (BH) divers, given its ability to evoke profound hypoxemic-hypercapnia and compensatory adaptations that preserve bioenergetic homeostasis, affords a unique opportunity to address these knowledge gaps.

Extending prior work focused exclusively on BBB integrity[6], this study combined volumetric assessment of CBF with concurrent sampling of arterio-jugular venous concentration differences ($a\text{-}v_D$) to calculate cerebral exchange kinetics of intravascular OXNOS biomarkers

medRxiv preprint doi: https://doi.org/10.1101/2023.07.24.23293124; this version posted July 27, 2023. The copyright holder for this preprint
(which was not certified by peer review) is the author/funder, who has granted medRxiv a license to display the preprint in perpetuity.
It is made available under a CC-BY-NC-ND 4.0 International license .

in world-class apneists over the course of two maximal, static apneas performed in ambient air. The first was performed following (standard) prior normoxic normoventilation resulting in severe hypoxemia-hypercapnia apnea (HHA) whereas the second followed prior hyperoxic hyperventilation, designed to prevent hypoxemia resulting in isolated hypercapnic apnea (IHA). By manipulating arterial O_2 independent of CO_2 tension, we sought to address the following hypotheses (Figure 1A). First, that cerebral output [venous (v) > arterial (a)] of free radicals and suppression of NO metabolite consumption and CBF would be more pronounced in the normoxic (HHA) compared to hyperoxic (IHA) apnea, implicating hypoxemia as the dominant OXNOS catalyst. Second that the apnea-induced elevation in CBF would be proportional to a net loss (a > v) of NO_2^- and SNO-Hb taken to reflect metabolite consumption and delivery of NO.

medRxiv preprint doi: https://doi.org/10.1101/2023.07.24.23293124; this version posted July 27, 2023. The copyright holder for this preprint (which was not certified by peer review) is the author/funder, who has granted medRxiv a license to display the preprint in perpetuity. It is made available under a CC-BY-NC-ND 4.0 International license .

METHODS

Ethics

Experimental procedures were approved by the University of Split, Ethics Committee (#H14-00922). All procedures were carried out in accordance with the most (7^{th}) recent amendment of the Declaration of Helsinki of the World Medical Association[7] (with the exception that it was not registered in a publicly accessible database prior to recruitment) with verbal and written informed consent obtained from all participants.

Participants

Ten physically active, elite apneists (6 men, 4 women) aged 33 (mean) ± 9 (SD) years old with a body mass index of 23 ± 2 kg/m^2 and forced vital capacity of 6.40 ± 1.48 L volunteered from the Croatian National Apnea Team. At the time of these experiments, six had placed within the world's top 10 within the last 5 years. One female set a new official world record in dynamic apnea while another male set the world record for apnea following prior hyperoxic hyperventilation (24 min 33 s). A medical examination confirmed that all participants were free of cardiovascular, pulmonary and cerebrovascular disease and were not taking any nutritional supplements including over-the-counter antioxidant or anti-inflammatory medications. They were advised to refrain from physical activity, caffeine and alcohol for 24 h prior to formal experimentation and maintain their normal dietary behavior. Participants attended the laboratory following a 12 h overnight fast.

Design

Parts of this study including blood gas and select aspects of cerebral hemodynamic function (Supplementary material Tables 1-2) have previously been published as part of separate

medRxiv preprint doi: https://doi.org/10.1101/2023.07.24.23293124; this version posted July 27, 2023. The copyright holder for this preprint (which was not certified by peer review) is the author/funder, who has granted medRxiv a license to display the preprint in perpetuity. It is made available under a CC-BY-NC-ND 4.0 International license .

investigations focused on the link between hypercapnia and cerebral oxidative metabolism[8] and hyper-perfusion-mediated structural destabilization of the NVU[6]. Thus, although the present study adopted an identical experimental design, it constitutes an entirely separate investigation complemented by *de novo* experimental measures and *a priori* hypotheses focused exclusively on altered redox homeostasis. Participants were required to perform two maximal apneas preceded by, [1] normoxic normoventilation resulting in severe hypoxemic hypercapnia apnea (HHA) and [2] hyperoxic hyperventilation designed to prevent hypoxemia resulting in isolated hypercapnic apnea (IHA). The order of trials was non-randomized given the long-lasting carryover effects of hyperoxia and fatigue associated with a more prolonged apnea[8]. Data were collected at baseline and timed to coincide with the point of apnea termination (Figure 1B).

Procedures

All apneas were completed on a single day with the Croatian national apnea coach present to motivate divers and ensure maximal efforts. Each apnea was preceded by 30 min of supine rest followed by two standardized preparatory (practice) apneas designed to maximize the experimental apneas (see below). The first preparatory apnea was performed at functional residual capacity (FRC) until seven involuntary breathing movements (IBMs) were attained. Two minutes later, the second preparatory apnea was performed at total lung capacity (TLC) lasting for ten IBMs. Participants then rested quietly for 6 min prior to two 'maximal' apneas that were each performed at TLC:

medRxiv preprint doi: https://doi.org/10.1101/2023.07.24.23293124; this version posted July 27, 2023. The copyright holder for this preprint (which was not certified by peer review) is the author/funder, who has granted medRxiv a license to display the preprint in perpetuity. It is made available under a CC-BY-NC-ND 4.0 International license .

Trial 1: Prior normoxic normoventilation- hypoxemic hypercapnia apnea (HHA)

Participants performed a maximal apnea in room air (normoxia).

Trial 2: Prior hyperoxic hyperventilation- isolated hypercapnic apnea (IHA)

Participants performed a maximal apnea preceded by 15 min of hyperventilation of 100% O_2 while receiving auditory feedback from the coach to achieve an end tidal PCO_2 (PET_{CO2}) of ~20 mmHg.

Blood sampling

Catheterization

Participants were placed slightly head down on a hospital bed, and two catheters were inserted retrograde using the Seldinger technique under local anesthesia (1 % lidocaine) via ultrasound guidance. A 20-guage arterial catheter (Arrow, Markham, ON, Canada) was placed in the right radial artery (a) and attached to an in-line waste-less sampling setup (Edwards Lifesciences VAMP, CA, USA) connected to a pressure transducer that was placed at the height of the right atrium (TruWave transducer). A central venous catheter (Edwards PediaSat Oximetry Catheter, CA, USA) was placed in the right internal jugular vein (v) and advanced towards the jugular bulb located at the mastoid process, approximately at the C1-C2 interspace (Figure 1). Facial vein contamination was ruled out by ensuring that all jugular venous oxyhemoglobin saturation (SO_2) values were < 75% at rest. Participants rested for at least 30 min following catheter placement prior to the collection of baseline samples.

medRxiv preprint doi: https://doi.org/10.1101/2023.07.24.23293124; this version posted July 27, 2023. The copyright holder for this preprint (which was not certified by peer review) is the author/funder, who has granted medRxiv a license to display the preprint in perpetuity. It is made available under a CC-BY-NC-ND 4.0 International license .

176 *Collection and storage*

177 Blood samples were drawn without stasis simultaneously from the RA and JV directly into
178 Vacutainers (Becton, Dickinson and Company, Oxford, UK) before centrifugation at 600g (4°C)
179 for 10 min. With the exception of blood for determination of blood gas variables, plasma and
180 red blood cell (RBC) samples were decanted into cryogenic vials (Nalgene Labware, Thermo
181 Fisher Scientific Inc, Waltham, MA) and immediately snap-frozen in liquid nitrogen (N_2)
182 before transport under nitrogen gas (Cryopak, Taylor-Wharton, Theodore, AL) from Croatia
183 to the United Kingdom. Samples were left to defrost at 37°C in the dark for 5 minutes prior to
184 batch analysis.

185

186 Measurements

187 *Blood gases*

188 Whole blood was collected into heparinized syringes, maintained anerobically at room
189 temperature and immediately analyzed for hemoglobin (Hb), hematocrit (Hct), partial
190 pressures of oxygen, carbon dioxide (PO_2/PCO_2), SO_2, pH and glucose (Glu) using a
191 commercially available cassette-based analyzer (ABL-90 FLEX, Radiometer, Copenhagen,
192 Denmark). Hydrogen ion (H^+) concentration was calculated as $[H^+] = 10^{-pH}$. The intra- and
193 inter-assay CVs for all metabolites were both <5%[9].

194

195 *Antioxidants*

196 Plasma was stabilized and deproteinated using 10% metaphosphoric acid (Sigma Chemical,
197 Dorset, UK). Ascorbic acid was assayed by fluorimetry based on the condensation of
198 dehydroascorbic acid with 1,2-phenylenediamine[10]. Concentrations of the lipid soluble
199 antioxidants (LSA) encompassing α/γ-tocopherol, α/β-carotene, retinol and lycopene were

medRxiv preprint doi: https://doi.org/10.1101/2023.07.24.23293124; this version posted July 27, 2023. The copyright holder for this preprint (which was not certified by peer review) is the author/funder, who has granted medRxiv a license to display the preprint in perpetuity. It is made available under a CC-BY-NC-ND 4.0 International license .

200 determined using high-performance liquid chromatography (HPLC)[11, 12]. The intra- and inter-
201 assay CVs for both metabolites were both <5%[9].

202 *Free radicals*

203 *Ascorbate free radical ($A^{\cdot-}$)*: We employed electron paramagnetic resonance (EPR)
204 spectrosopic detection of $A^{\cdot-}$ as a direct measure of global systemic free radical formation[9].
205 Plasma (1 mL) was injected directly into a high-sensitivity multiple-bore sample cell (AquaX,
206 Bruker Daltonics Inc., Billerica, MA, USA) housed within a TM_{110} cavity of an EPR
207 spectrometer operating at X-band frequency (9.87 GHz). Samples were recorded by
208 cumulative signal averaging of 10 scans using the following instrument parameters:
209 resolution, 1024 points: microwave power, 20 mW; modulation amplitude, 0.65 G; receiver
210 gain, 2×10^6; time constant, 40.96 ms; sweep rate, 0.14 G/s; sweep width, 6 G; centre field,
211 3486 G. All spectra were filtered identically (moving average, 15 conversion points) using
212 WINEPR software (Version 2.11, Bruker, Karlsruhe, Germany) and the double integral of each
213 doublet quantified using Origin 8 software (OriginLab Corps, MA, USA). The intra- and inter-
214 assay CVs were both <5%[9].

215

216 *Lipid hydroperoxides (LOOH)*: LOOH were determined spectrophotometrically via the ferric
217 oxidation of xylenol orange (FOX) version II method, with modification[9]. Intra- and inter-assay
218 CVs were <2 % and <4 % respectively[9].

219

220 *Nitric oxide (NO) metabolites*

221 Ozone-based chemiluminescence (Sievers NOA 280i, Analytix Ltd, Durham, UK) was used to
222 detect NO liberated from plasma and RBC samples via chemical reagent cleavage facilitating
223 detection of plasma and red blood cell (RBC) NO_2^-, *S*-nitrosothiols (RSNO), *S*-

medRxiv preprint doi: https://doi.org/10.1101/2023.07.24.23293124; this version posted July 27, 2023. The copyright holder for this preprint (which was not certified by peer review) is the author/funder, who has granted medRxiv a license to display the preprint in perpetuity. It is made available under a CC-BY-NC-ND 4.0 International license .

nitrosohemoglobin (SNO-Hb) and iron nitrosylhemoglobin (HbNO) according to established methods[13-15]. Total NO bioactivity was calculated as the cumulative concentration of plasma and RBC metabolites. Signal output was plotted against time using Origin 8 software (OriginLab Corps, Massachusetts, USA) and smoothed using a 150-point averaging algorithm. The Peak Analysis package was used to calculate the area under the curve and subsequently converted to a concentration using standard curves of sodium NO_2^-. Intra- and inter-assay CVs for all metabolites were both <10%[13].

Cardiopulmonary function

All cardiopulmonary measurements were averaged over 15 s immediately prior to blood sampling. A lead II electrocardiogram (Dual BioAmp; ADInstruments, Oxford, UK) was used to measure heart rate (HR). Intra-arterial ABP was recorded directly via a pressure transducer placed at the level of the heart for determination of mean arterial pressure (MAP). Internal jugular venous pressure (IJVP) was measured with the transducer connected to the jugular catheter. End-tidal partial pressures of oxygen and carbon dioxide ($PET_{O2/CO2}$) were measured via capnography (ML 206, ADInstruments Ltd, Oxford, UK). Finger photoplethysmography (Finometer PRO, Finapres Medical Systems, Amsterdam, The Netherlands) was used to measure beat-by-beat stroke volume (SV) and cardiac output ($\dot{Q}$) using the Modelflow algorithm[16] that incorporates participant sex, age, stature and mass (BeatScope 1.0 software; TNO; TPD Biomedical Instrumentation, Amsterdam, The Netherlands).

Cerebrovascular function

Intracranial: Blood velocity in the middle cerebral artery (MCAv, insonated through the left temporal window and posterior cerebral artery (PCAv, insonated at the P1 segment through

medRxiv preprint doi: https://doi.org/10.1101/2023.07.24.23293124; this version posted July 27, 2023. The copyright holder for this preprint (which was not certified by peer review) is the author/funder, who has granted medRxiv a license to display the preprint in perpetuity. It is made available under a CC-BY-NC-ND 4.0 International license .

the right temporal window) were measured using standardized procedures with a 2 MHz pulsed transcranial Doppler ultrasound (TCD; Spencer Technologies, Seattle, WA, USA). Bilateral TCD probes were secured using a specialized commercial headband (Mark600, Spencer Technologies, Seattle, WA, USA) using standardized search techniques.

Extracranial: Continuous diameter, velocity and blood flow recordings in the right internal carotid and left vertebral arteries ($\dot{Q}_{ICA}$/$\dot{Q}_{VA}$) were obtained using a 10 MHz, multifrequency, linear array vascular ultrasound (Terason 3200, Teratech, Burlington, MA). Arterial diameter was measured via B-mode imaging, whereas peak blood velocity was simultaneously measured with pulse-wave mode. The ICA was insonated ≥1.5 cm from the carotid bifurcation, with no evidence of turbulent or retrograde flow present during recording. The VA was insonated at the C4–C5 or C5–C6 vertebral segment and standardized within participants for the HHA and IHA trials. The steering angle was fixed to 60° and the sample volume was placed in the center of the vessel and adjusted to cover the entire vascular lumen. All images were recorded as video files at 30 Hz and stored for offline analysis using customized edge detection software designed to mitigate observer bias[17]. Simultaneous measures of arterial diameter and velocity over >12 consecutive cardiac cycles were used to calculate flow. Between-day CVs for $\dot{Q}_{ICA}$ and $\dot{Q}_{VA}$ are 5 % and 11 %, respectively[18].

Data integration

All cardiopulmonary measurements were sampled at 1 kHz and integrated into PowerLab® and LabChart® software (ADInstruments, Bella Vista, NSW, Australia) for online monitoring and saved for offline analysis.

medRxiv preprint doi: https://doi.org/10.1101/2023.07.24.23293124; this version posted July 27, 2023. The copyright holder for this preprint (which was not certified by peer review) is the author/funder, who has granted medRxiv a license to display the preprint in perpetuity. It is made available under a CC-BY-NC-ND 4.0 International license .

Calculations

Cerebral bioenergetics

Perfusion: Volumetric blood flow was calculated offline as:

$$\dot{Q}_{ICA} \text{ or } \dot{Q}_{VA} \text{ (mL/min)} = \frac{\text{peak envelope blood velocity}}{2} \times [\pi(0.5 \times \text{diameter})^2] \times 60$$

$\dot{Q}_{ICA}$ or $\dot{Q}_{VA}$ were averaged for a 1 min eupnea baseline and during the last 30 s of apnea.

During the latter half of each apnea, IBMs and corresponding contraction of the sternocleidomastoid prevented reliable blood velocity traces. To circumvent this, Q_{ICA} and Q_{VA} were estimated (e) from changes in MCAv (for $\dot{Q}_{ICA}$) and PCAv (for $\dot{Q}_{VA}$) respectively, as previously described[19, 20]:

$$\text{Apnea eICAv and eVAv} = \text{Eupnea ICAv and VAv} \times \left(\frac{\text{Apnea MCAv or PCAv}}{\text{Eupnea MCAv or PCAv}}\right)$$

$$\dot{Q}_{ICA} \text{ or } \dot{Q}_{VA} \text{ (mL/min)} = \text{eICAv or eVAv} \times \pi\left(\frac{\text{diameter}}{2}\right)^2$$

Assuming symmetrical blood flow of contralateral ICA and VA arteries, global cerebral blood flow (gCBF) was calculated as:

$$\text{gCBF (mL/min)} = 2 \times (\dot{Q}_{ICA} + \dot{Q}_{VA})$$

Cerebral perfusion pressure (CPP) was calculated as MAP-IJVP with the latter serving as a surrogate for ICP[21].

medRxiv preprint doi: https://doi.org/10.1101/2023.07.24.23293124; this version posted July 27, 2023. The copyright holder for this preprint (which was not certified by peer review) is the author/funder, who has granted medRxiv a license to display the preprint in perpetuity. It is made available under a CC-BY-NC-ND 4.0 International license .

Metabolism: Arterial and jugular venous oxygen content (caO_2 and cvO_2 respectively) were calculated as:

$$caO_2\ (mL/dL) = Hb\ (g/dL) \times 1.34\left(\frac{SaO_2\ (\%)}{100}\right) + 0.003 \times PaO_2$$

$$cvO_2\ (mL/dL) = Hb\ (g/dL) \times 1.34\left(\frac{SvO_2\ (\%)}{100}\right) + 0.003 \times PvO_2$$

where 1.34 is the O_2 binding capacity of Hb and 0.003 is the solubility of O_2 dissolved in blood.

Global cerebral O_2 and glucose delivery ($gCDO_2$/$gCD_{Glucose}$) were calculated as:

$$gCDO_2\ (mL/min) = \left(\frac{gCBF\ (mL/min}{100}\right) \times caO_2\ (mL/dL)$$

$$gCD_{Glu}\ (mmol/min) = \left(\frac{gCBF\ (mL/min}{1000}\right) \times a_{Glucose}\ (mmol/L)$$

The cerebral metabolic rate of oxygen ($CMRO_2$) and glucose ($CMR_{Glucose}$) were calculated as:

$$CMRO_2\ (mL/min) = \left(\frac{gCBF\ (mL/min}{100}\right) \times caO_2\text{-}cvO_2\ (mL/dL)$$

$$CMR_{Glucose}\ (mmol/min) = \left(\frac{gCBF\ (mL/min}{1000}\right) \times a_{Glucose} - v_{Glucose}\ (mmol/L)$$

Transcerebral exchange kinetics

gCBF was converted into global cerebral plasma (gCPF) and red blood cell (gCRBCF) flow:

$$gCPF\ (mL/min) = gCBF\left(1 - \frac{Hct_a}{100}\right)$$

medRxiv preprint doi: https://doi.org/10.1101/2023.07.24.23293124; this version posted July 27, 2023. The copyright holder for this preprint (which was not certified by peer review) is the author/funder, who has granted medRxiv a license to display the preprint in perpetuity. It is made available under a CC-BY-NC-ND 4.0 International license .

317

318 $\text{gCRBCF (mL//min)} = \text{gCBF}\left(\frac{\text{Hct}_a}{100}\right)$

319 for corresponding calculation of net transcerebral exchange kinetics of plasma/serum/RBC-

320 borne metabolites according to the Fick principle:

321

322 Exchange (µmol or nmol/min) = gCBF or gCPF or gCRBCF × $(a - v_D)$.

323 By convention, a positive value (a>v) refers to net uptake (loss or consumption) whereas a

324 negative value (v>a) indicates net output (gain or formation) across the cerebrovascular bed.

325

326 ## Data analysis

327 Data were analyzed using the Statistics Package for Social Scientists (IBM SPSS Statistics

328 Version 29.0). Distribution normality was confirmed using Shapiro-Wilk *W* tests ($P > 0.05$).

329 Data were analyzed using a combination of two (*State*: Eupnea *vs*. Apnea × *Site*: Arterial *vs*.

330 Venous) and three (*Trial*: HHA *vs*. IHA × *State*: Eupnea *vs*. Apnea × *Site*: Arterial *vs*. Venous)

331 factor repeated measures analyzes of variance. Post-hoc Bonferroni-corrected paired

332 samples *t*-tests were employed to locate differences following an interaction. Relationships

333 between selected variables were analyzed using Pearson Product Moment Correlations.

334 Significance was established at $P < 0.05$ for all two-tailed tests and data presented as mean ±

335 SD.

336

medRxiv preprint doi: https://doi.org/10.1101/2023.07.24.23293124; this version posted July 27, 2023. The copyright holder for this preprint (which was not certified by peer review) is the author/funder, who has granted medRxiv a license to display the preprint in perpetuity. It is made available under a CC-BY-NC-ND 4.0 International license .

RESULTS

Apnea

Apnea duration increased from 306 ± 62 s (range: 217-409 s) during HHA to 959 ± 201 s (range: 579-1262 s) during IHA (P = <0.001).

Blood gas variables

As expected, apnea induced severe systemic and local hypoxemia ($\downarrow PO_2$, $\downarrow SO_2$, $\downarrow cO_2$), hypercapnia ($\uparrow PCO_2$) and acidosis ($\downarrow$pH, $\uparrow HCO_3^-$) in NX (Supplemental Table 1). In one participant, nadirs of 29 mmHg and 40 % were recorded for PaO_2 and SaO_2 respectively, corresponding to a (peak) $PaCO_2$ of 53 mmHg in HHA. Participants were hypocapnic at eupnea in IHA and remained hyperoxemic and comparatively less hypertensive and more hypercapnic/acidotic throughout apnea (Supplemental Table 1). The highest individual value recorded for $PaCO_2$ during IHA was 68 mmHg corresponding to a pH of 7.227. Baseline levels of Hb and Hct at eupnea were elevated in IHA (Supplemental Table 1).

Cardiopulmonary function

Apnea decreased SV and $\dot{Q}$ in HHA whereas increases were observed in IHA (Table 1). Apnea was associated with a general increase in MAP, IJVP and CPP that were more pronounced in HHA (Supplemental Table 1).

Cerebral bioenergetics

Compared to the eupnic control states (normoxic normocapnia), a greater increase in gCBF was observed in IHA (+206 ± 52 %) compared to HHA (+83 ± 22 %, *P* = <0.001) due to consistently lower $\dot{Q}_{ICA}$ and $\dot{Q}_{VA}$ values at baseline subsequent to (hyperoxic)

medRxiv preprint doi: https://doi.org/10.1101/2023.07.24.23293124; this version posted July 27, 2023. The copyright holder for this preprint (which was not certified by peer review) is the author/funder, who has granted medRxiv a license to display the preprint in perpetuity. It is made available under a CC-BY-NC-ND 4.0 International license .

hyperventilation-induced hypocapnia (Supplemental Table 3). Corresponding increases in local (VA/ICA) and global cerebral substrate delivery (O_2 and glucose) were also more pronounced during apnea in IHA (Supplemental Table 3). Apnea generally decreased $CMRO_2$ whereas CMR_{Glu} remained preserved with no differences between trials (Supplemental Table 3).

Oxidative stress

Apnea increased the a-v_D and corresponding net cerebral uptake of ascorbate, α-tocopherol and total LSA that were more pronounced in HHA (Table 1, Figure 2 A-C). This was accompanied by a reduction in the a-v_D and reciprocal elevation in the net cerebral output of $A^{\cdot-}$ and LOOH that were also more marked in HHA for $A^{\cdot-}$ (Table 1, Figure 2 D-E).

Nitrosative stress

Figure 3 highlights the dynamic interplay and re-apportionment of NO metabolites across the cerebral circulation observable within the constraints of a single a-v transit. The total NO metabolite pool was generally lower in HHA and during apnea due to a combined reduction in plasma and RBC NO_2^- whereas elevations were observed in SNO-Hb and HbNO (Table 2, Figure 3). Corresponding differences translated into net cerebral uptake of plasma NO_2^-, RSNO and RBC NO_2^- (Figure 4 A-B, D) that were opposed by net cerebral output of SNO-Hb and HbNO (Figure 4 E-F). Plasma NO_2^- uptake and SNO-Hb/HbNO output were more pronounced during apnea, with plasma NO_2^- uptake generally lower in HHA (Figure 4 A, E-F). The apnea-induced elevation in $A^{\cdot-}$ output was associated with a reduction in plasma NO_2^- uptake in HHA ($r = 0.702$, $P = 0.024$) but not IHA ($r = 0.509$, $P = 0.133$).

medRxiv preprint doi: https://doi.org/10.1101/2023.07.24.23293124; this version posted July 27, 2023. The copyright holder for this preprint (which was not certified by peer review) is the author/funder, who has granted medRxiv a license to display the preprint in perpetuity. It is made available under a CC-BY-NC-ND 4.0 International license .

DISCUSSION

Local sampling of blood across the cerebral circulation during maximal apnea in world-class BH divers has provided important insight into the mechanisms underlying the redox-regulation of cerebral bioenergetic function during the most severe extremes of O_2 demand/CO_2 production recorded to date in unanesthetized and otherwise healthy humans[22]. Direct measures of intravascular OXNOS and inclusion of the IHA trial designed to prevent hypoxemia and better distinguish between competing vasoactive stimuli, highlights three novel findings. First, the combined elevation in the net cerebral output of $A^{\cdot-}$ and LOOH during apnea, collectively taken to reflect increased free radical-mediated lipid peroxidation, was more pronounced in HHA, highlighting a key contribution for hypoxemia. Second, this coincided with a lower apnea-induced elevation in gCBF and related suppression in plasma NO_2^- uptake, implying reduced consumption and delivery of NO consistent with increased OXNOS. Finally, that apnea-induced NO_2^- uptake and HbNO output prevailed in the face of increased SNO-Hb output and (general) RSNO uptake, tentatively suggests NO_2^- reduction as the more likely mechanism underlying endocrine NO vasoregulation with the capacity to transduce physiological O_2-CO_2 gradients into graded vasodilation. Collectively, these findings highlight the dynamic interplay that takes place between free radicals and NO metabolites during a single arteriovenous transit across the cerebral circulation and corresponding implications for cerebral bioenergetic function that may have clinical translational relevance.

Hypoxemia is a key stimulus for cerebral OXNOS

We recently documented molecular evidence for structural destabilization of the NVU that was selectively more pronounced during apnea in HHA compared to IHA despite

medRxiv preprint doi: https://doi.org/10.1101/2023.07.24.23293124; this version posted July 27, 2023. The copyright holder for this preprint (which was not certified by peer review) is the author/funder, who has granted medRxiv a license to display the preprint in perpetuity. It is made available under a CC-BY-NC-ND 4.0 International license .

comparatively suppressed, albeit concerted vasodilation[6]. While this was originally attributed purely to the 'mechanical' stress imposed by more severe systemic and intracranial hypertension caused by hypoxemia, the present findings suggest a potentially additive role for 'chemical' stress, taking the form of elevated OXNOS, to which the human brain is especially vulnerable.

To do this, we employed EPR spectroscopic detection of the distinctive $A^{\cdot-}$ 'doublet' as a direct biomarker of global free radical formation with LOOH serving as a distal reactant of lipid peroxidation[9]. That net cerebral uptake (a>v) of ascorbate, α-tocopherol and (total) LSA was observed during apnea in both trials, and more pronounced in HHA, was taken to reflect enhanced sacrificial consumption (uptake by brain parenchyma and/or blood-borne reactions during circulatory transit) to constrain chain initiation-propagation reactions. However, this failed to prevent the overall shift in redox imbalance favouring increased free radical-mediated lipid peroxidation confirmed by proportional increases in the net cerebral output of $A^{\cdot-}$ and LOOH (v>a) that were selectively elevated in HHA. The greater elevation in $A^{\cdot-}$ output in HHA exceeded that predicted by prior modelling due to more ascorbate available for oxidation[23] (given increased consumption), highlighting authentic (i.e. *de novo*) free radical formation. Our measured $A^{\cdot-}$ gradients in HHA (v = 37 % > a) also exceeded those previously recorded during HHA in a separate group of elite apneists[24] (v = 4 % > a) and were even more pronounced than those documented during vigorous cycling exercise[9] (v = 12 % > a) - helping place its magnitude into clearer physiological context.

While it is conceivable that hypoxemia, hypercapnia and hyperoxemia independently contributed towards global oxidative stress, it was not experimentally possible to fully differentiate between stimuli, only combinations thereof. Hypoxemia and hyperoxemia independently generate mitochondrial superoxide ($O_2^{\cdot-}$) and $NO^{\cdot}$, notwithstanding

medRxiv preprint doi: https://doi.org/10.1101/2023.07.24.23293124; this version posted July 27, 2023. The copyright holder for this preprint (which was not certified by peer review) is the author/funder, who has granted medRxiv a license to display the preprint in perpetuity. It is made available under a CC-BY-NC-ND 4.0 International license .

contributions from extra-mitochondrial sources including nicotinamide adenine dinucleotide phosphate- and xanthine oxidases, cytochrome P-450 enzymes, lipoxygenases and phagocytes, that can further propagate oxidative stress via secondary formation of hydrogen peroxide (H_2O_2), peroxynitrite ($ONOO^-$) and Haber-Weiss/Fenton catalyzed hydroxyl radicals ($OH^{\cdot-}$)[25, 26]. Furthermore, the addition of (hypercapnic) acidosis, common to both trials yet more severe in HX given the extended BH times, would have been expected to further amplify oxidation since molecular CO_2 can react with $ONOO^-$ and H_2O_2 to form redox reactive carbonate radicals and peroxymonocarbonate[27]. However, that cerebral oxidative stress was considerably more pronounced in HHA suggests a key catalytic role for hypoxemia that far outweighed the additive effects of hyperoxemia and (more severe) hypercapnia, confirming prior observations in healthy humans albeit exposed to poikilocapnic (hypocapnic) hypoxia[9, 28].

To what extent this represents a physiologically adaptive (molecular signalling) or pathologically maladaptive (structurally damaging) response remains unclear given the pleiotropic mechanisms underlying redox-regulation of NVU function[4]. That oxidative stress was elevated in the face of reduced $gCMRO_2$ and $gCMR_{Glucose}$, attributable in part to hypercapnia[8], has also been observed in (more) anoxia–hypoxia-tolerant vertebrates and interpreted to reflect an adaptive O_2-conserving strategy to improve neuronal survival[29].

However, two observations in the present study tentatively suggest that the overall impact was likely maladaptive. First, that apnea in NX was associated with a lower net uptake of plasma NO_2^- implied reduced consumption of NO, potentially tempering vasodilation (see below). This may reflect oxidative inactivation of NO by $O_2^{\cdot-}$ and/or secondary lipid-derived alkoxyl-alkyl radicals formed subsequent to the reductive decomposition of (elevated) LOOH

medRxiv preprint doi: https://doi.org/10.1101/2023.07.24.23293124; this version posted July 27, 2023. The copyright holder for this preprint (which was not certified by peer review) is the author/funder, who has granted medRxiv a license to display the preprint in perpetuity. It is made available under a CC-BY-NC-ND 4.0 International license .

454 to form $ONOO^-$, collectively taken as evidence for elevated OXNOS ($O_2^{\cdot-}/LO^{\cdot}/LC^{\cdot}$ + NO $\xrightarrow{10^9 M/s}$
455 $ONOO^-$)[30]. Second, that our prior research has shown that apnea induces mild disruption of
456 the BBB and increased neuronal-gliovascular reactivity that were consistently more
457 pronounced in HHA[6], stands testament to the thermodynamic potential of radicals to cause
458 structural damage to the NVU, which is not unreasonable given its histological vulnerability[4,
459 31].

460

461 ## NO metabolites and vasoregulation

462 Our findings highlight that the NO metabolite pool is in a perpetual state of dynamic flux
463 even within the time constraints of a single a-v transit and that metabolite re-apportionment
464 between plasma and RBC compartments is not solely related to changes in O_2 but also
465 involves CO_2 and pH (Figure 3). By measuring corresponding gradients of NO_2^- and SNO-Hb,
466 the principal metabolites capable of transducing NO bioactivity within the cerebral
467 microcirculation[32, 33], we sought to determine if differential changes could further inform the
468 mechanism(s) underlying cerebral vasodilation across extremes of PaO_2 and $PaCO_2$. Both
469 metabolites likely originated from the combined effects of apnea-induced elevations in
470 shear-mediated conduit vessel endothelial[34], neuronal[35] NO synthase bioactivation and
471 transpulmonary *S*-nitrosylation[32]; however, their respective roles in endocrine NO signalling
472 and cerebral bioenergetic function remain widely contested, albeit unified by allosteric-
473 coupled Hb deoxygenation and acidic disproportionation[5].

474 The NO_2^- reductase hypothesis favors NO_2^- as the major intravascular NO storage molecule
475 with conversion to NO or dinitrogen trioxide (N_2O_3) catalyzed by deoxyHb-mediated
476 reduction and acidic disproportionation[13, 33, 36]. In contrast, the SNO-Hb hypothesis contends

medRxiv preprint doi: https://doi.org/10.1101/2023.07.24.23293124; this version posted July 27, 2023. The copyright holder for this preprint (which was not certified by peer review) is the author/funder, who has granted medRxiv a license to display the preprint in perpetuity. It is made available under a CC-BY-NC-ND 4.0 International license .

that NO is stabilized, transported, and delivered by intra-molecular NO group transfers between the heme iron and β-93 cysteine, that upon deoxygenation releases an as of yet unidentified moiety that is exported from the RBC involving transnitrosylation of the anion exchanger AE1, as a low molecular weight RSNO to effect vasodilation[32, 37, 38].

The direction and magnitude of gradients observed are generally more consistent with those predicted by the NO_2^- reductase (as opposed to the SNO-Hb) hypothesis. In support, systemic (a) plasma NO_2^- fell during apnea and was accompanied by a concomitant increase in net uptake implying consumption from artery to vein (a>v), although we cannot discount consistently elevated NO_2^- formation on the arterial side due to elevated NOS activity. Plasma NO_2^- consumption was especially marked in HX, coinciding with the most pronounced elevation in gCBF and where the total NO metabolite pool was greatest. This was accompanied by NO formation with concomitant output (v>a) of HbNO, albeit suppressed in IHA consistent with the prevailing SO_2 since hyperoxemia persisted at end apnea, culminating in an overall net gain in NO metabolites. These findings were taken to reflect a combination of deoxyHb-mediated reduction of NO_2^- in the RBC and acidic disproportionation subsequent to marked hypercapnia-induced acidosis. Local formation of NO, potentially compounded by the observed increase in ascorbate consumption[39], binds to vicinal deoxyHb yielding HbNO (Equations 1 and 2) and, to a lesser extent, the intermediate nitrosating species dinitrogen trioxide that can escape the RBC to effect graded vasodilation[33]:

$$NO_2^- + HbFe^{2+}(\text{deoxyHb}) + H^+ \xrightarrow{0.47\ M/s} HbFe^{3+}(\text{metHb}) + NO + OH^- \quad \text{(Equation 1)}$$

$$NO + HbFe^{2+} \xrightarrow{0.18\ M/s} HbFe^{2+}NO\ (\text{HbNO}) \quad \text{(Equation2)}$$

medRxiv preprint doi: https://doi.org/10.1101/2023.07.24.23293124; this version posted July 27, 2023. The copyright holder for this preprint (which was not certified by peer review) is the author/funder, who has granted medRxiv a license to display the preprint in perpetuity. It is made available under a CC-BY-NC-ND 4.0 International license .

The gradients observed reproduce those previously documented across the exercising human forearm circulation and NO_2^- infusion that originally informed the NO_2^- reductase hypothesis[33, 36]. Similar gradients were more recently documented across the cerebral circulation at rest and in response to acute exercise during hypocapnic hypoxia[13].

In contrast, that apnea stimulated SNO-Hb output (v>a) and RSNO uptake (a>v) argues against the SNO-Hb hypothesis, since the gradients observed were diametrically opposed to those originally predicted[40], yet consistent with the observations of other research laboratories[41, 42]. We would have expected an allosterically mediated release from a-v during circulatory transit, resulting in a drop in the RBC and corresponding rise in plasma RSNO in the venous circulation, consistent with SNO-Hb consumption (a>v) and RSNO delivery (v>a) during local deoxygenation. Yet, the gradients observed consistently reflected SNO-Hb formation (v>a) and RSNO consumption (a>v), that in the former, was further compounded during apnea and unrelated to the increase in gCBF.

Experimental limitations

Several limitations warrant consideration. First, it was not possible to fully disassociate changes in PaO_2 from $PaCO_2$, only combinations thereof, given the inability to 'match' end-apnea hypercapnia that was unavoidably more pronounced in HX owing to extended BH times. Second, it was unfortunate that we did not measure plasma 3-nitrotyrosine due to inadequate sample volume: its elevation would have indirectly confirmed increased $ONOO^-$ formation subsequent to oxidative inactivation of NO underlying OXNOS, consistent with our prior observations in hypoxia[35]. Third, the profiling of NO metabolite gradients, while informative, fails to unequivocally identify the specific NO species responsible for conserving

medRxiv preprint doi: https://doi.org/10.1101/2023.07.24.23293124; this version posted July 27, 2023. The copyright holder for this preprint
(which was not certified by peer review) is the author/funder, who has granted medRxiv a license to display the preprint in perpetuity.
It is made available under a CC-BY-NC-ND 4.0 International license .

bioactivity and the mechanism(s) underpinning vasoregulation, including potential contributions from ATP-mediated activation of P_{2Y} receptors. Finally, despite prospective power calculations informed by our prior research[24], we acknowledge the small sample sizes employed may have limited our ability to detect treatment effects, albeit challenging to perform large-scale invasive studies of this nature. Caveats notwithstanding, mapping the dynamic transvascular interplay of OXINOS biomarkers in this applied model of human asphyxia may prove clinically relevant in that it may help define more sensitive biomarkers of cerebrovascular health and inform interventions designed to optimize tissue oxygenation in the critically ill.

medRxiv preprint doi: https://doi.org/10.1101/2023.07.24.23293124; this version posted July 27, 2023. The copyright holder for this preprint (which was not certified by peer review) is the author/funder, who has granted medRxiv a license to display the preprint in perpetuity. It is made available under a CC-BY-NC-ND 4.0 International license .

REFERENCES

1. Schaeffer S and Iadecola C. Revisiting the neurovascular unit. *Nat Neurosci*. 2021;24:1198-1209.

2. Rinaldi C, Donato L, Alibrandi S, Scimone C, D'Angelo R and Sidoti A. Oxidative Stress and the Neurovascular Unit. *Life (Basel)*. 2021;11.

3. Bailey DM. Oxygen, evolution and redox signalling in the human brain; quantum in the quotidian. *The Journal of physiology*. 2019;597:15-28.

4. Cobley JN, Fiorello ML and Bailey DM. 13 reasons why the brain is susceptible to oxidative stress. *Redox biology*. 2018;15:490-503.

5. Gladwin MT and Schechter AN. NO contest: nitrite versus S-nitroso-hemoglobin. *Circulation Research*. 2004;94:851-5.

6. Bailey DM, Bain AR, Hoiland RL, Barak OF, Drvis I, Hirtz C, Lehmann S, Marchi N, Janigro D, MacLeod DB, Ainslie PN and Dujic Z. Hypoxemia increases blood-brain barrier permeability during extreme apnea in humans. *Journal of cerebral blood flow and metabolism : official journal of the International Society of Cerebral Blood Flow and Metabolism*. 2022;42:1120-1135.

7. WMA. World Medical Association Declaration of Helsinki: ethical principles for medical research involving human subjects. *Journal of the American Medical Association*. 2013;310:2191-4.

8. Bain AR, Ainslie PN, Barak OF, Hoiland RL, Drvis I, Mijacika T, Bailey DM, Santoro A, DeMasi DK, Dujic Z and MacLeod DB. Hypercapnia is essential to reduce the cerebral oxidative metabolism during extreme apnea in humans. *Journal of Cerebral Blood Flow and Metabolism*. 2017:271678X16686093.

medRxiv preprint doi: https://doi.org/10.1101/2023.07.24.23293124; this version posted July 27, 2023. The copyright holder for this preprint (which was not certified by peer review) is the author/funder, who has granted medRxiv a license to display the preprint in perpetuity. It is made available under a CC-BY-NC-ND 4.0 International license .

555 9. Bailey DM, Rasmussen P, Evans KA, Bohm AM, Zaar M, Nielsen HB, Brassard P,
556 Nordsborg NB, Homann PH, Raven PB, McEneny J, Young IS, McCord JM and Secher NH.
557 Hypoxia compounds exercise-induced free radical formation in humans; partitioning
558 contributions from the cerebral and femoral circulation. *Free Radical Biology & Medicine*
559 . 2018;124:104-113.
560 10. Vuilleumier JP and Keck E. Fluorimetric assay of vitamin C in biological materials using
561 a centrifugal analyser with fluorescence attachment. *Journal of Micronutritional Analysis*.
562 1993;5:25-34.
563 11. Catignani GL and Bieri JG. Simultaneous determination of retinol and alpha-
564 tocopherol in serum or plasma by liquid chromatography. *Clinical Chemistry*. 1983;29:708-
565 712.
566 12. Thurnham DI, Smith E and Flora PS. Concurrent liquid-chromatographic assay of
567 retinol, *a*-tocopherol, *b*-carotene, *a*-carotene, lycopene, and *b*-cryptoxanthin in plasma, with
568 tocopherol acetate as internal standard. *Clinical Chemistry*. 1988;34:377-381.
569 13. Bailey DM, Rasmussen P, Overgaard M, Evans KA, Bohm AM, Seifert T, Brassard P,
570 Zaar M, Nielsen HB, Raven PB and Secher NH. Nitrite and *S*-Nitrosohemoglobin exchange
571 across the human cerebral and femoral circulation: relationship to basal and exercise blood
572 flow responses to hypoxia. *Circulation*. 2017;135:166-176.
573 14. Rogers SC, Khalatbari A, Gapper PW, Frenneaux MP and James PE. Detection of
574 human red blood cell-bound nitric oxide. *Journal of Biological Chemistry*. 2005;280:26720-
575 26728.
576 15. Pinder AG, Rogers SC, Khalatbari A, Ingram TE and James PE. The measurement of
577 nitric oxide and its metabolites in biological samples by ozone-based chemiluminescence.
578 *Methods in molecular biology*. 2009;476:10-27.

medRxiv preprint doi: https://doi.org/10.1101/2023.07.24.23293124; this version posted July 27, 2023. The copyright holder for this preprint
(which was not certified by peer review) is the author/funder, who has granted medRxiv a license to display the preprint in perpetuity.
It is made available under a CC-BY-NC-ND 4.0 International license .

16. Wesseling KH, Jansen JR, Settels JJ and Schreuder JJ. Computation of aortic flow from pressure in humans using a nonlinear, three-element model. *Journal of applied physiology*. 1993;74:2566-73.

17. Woodman RJ, Playford DA, Watts GF, Cheetham C, Reed C, Taylor RR, Puddey IB, Beilin LJ, Burke V, Mori TA and Green D. Improved analysis of brachial artery ultrasound using a novel edge-detection software system. *Journal of applied physiology*. 2001;91:929-37.

18. Willie CK, Macleod DB, Shaw AD, Smith KJ, Tzeng YC, Eves ND, Ikeda K, Graham J, Lewis NC, Day TA and Ainslie PN. Regional brain blood flow in man during acute changes in arterial blood gases. *Journal of Physiology*. 2012;590:3261-75.

19. Hoiland RL, Ainslie PN, Bain AR, MacLeod DB, Stembridge M, Drvis I, Madden D, Barak O, MacLeod DM and Dujic Z. Beta1-Blockade increases maximal apnea duration in elite breath-hold divers. *Journal of applied physiology*. 2017;122:899-906.

20. Willie CK, Ainslie PN, Drvis I, MacLeod DB, Bain AR, Madden D, Maslov PZ and Dujic Z. Regulation of brain blood flow and oxygen delivery in elite breath-hold divers. *Journal of Cerebral Blood Flow and Metabolism*. 2015;35:66-73.

21. Myerson A and Loman J. Internal jugular venous pressure in man: Its relationship to cerebrospinal fluid and carotid arterial pressures. *Archives of Neurology and Psychiatry*. 1932;27:836–846.

22. Bailey DM, Willie CK, Hoiland RL, Bain AR, MacLeod DB, Santoro MA, DeMasi DK, Andrijanic A, Mijacika T, Barak OF, Dujic Z and Ainslie PN. Surviving without oxygen: how low can the human brain go? *High altitude medicine & biology*. 2017;18:73-79.

23. Fall L, Brugniaux JV, Davis D, Marley CJ, Davies B, New KJ, McEneny J, Young IS and Bailey DM. Redox-regulation of haemostasis in hypoxic exercising humans: a randomised

medRxiv preprint doi: https://doi.org/10.1101/2023.07.24.23293124; this version posted July 27, 2023. The copyright holder for this preprint
(which was not certified by peer review) is the author/funder, who has granted medRxiv a license to display the preprint in perpetuity.
It is made available under a CC-BY-NC-ND 4.0 International license .

602 double-blind placebo-controlled antioxidant study. *The Journal of physiology*. 2018;596:4879-
603 4891.
604 24. Bain AR, Ainslie PN, Hoiland RL, Barak OF, Drvis I, Stembridge M, MacLeod DM,
605 McEneny J, Stacey BS, Tuaillon E, Marchi N, De Maudave AF, Dujic Z, MacLeod DB and Bailey
606 DM. Competitive apnea and its effect on the human brain: focus on the redox regulation of
607 blood-brain barrier permeability and neuronal-parenchymal integrity. *FASEB journal : official*
608 *publication of the Federation of American Societies for Experimental Biology*. 2018;32:2305-
609 2314.
610 25. Turrens JF. Mitochondrial formation of reactive oxygen species. *Journal of Physiology*.
611 2003;552.2:335-344.
612 26. Murphy MP. How mitochondria produce reactive oxygen species. *The Biochemical*
613 *journal*. 2009;417:1-13.
614 27. Augusto O and Truzzi DR. Carbon dioxide redox metabolites in oxidative eustress and
615 oxidative distress. *Biophys Rev*. 2021;13:889-891.
616 28. Bailey DM, Taudorf S, Berg RMG, Lundby C, McEneny J, Young IS, Evans KA, James PE,
617 Shore A, Hullin DA, McCord JM, Pedersen BK and Moller K. Increased cerebral output of free
618 radicals during hypoxia: implications for acute mountain sickness? *American Journal of*
619 *Physiology (Regulatory, Integrative and Comparative Physiology)*. 2009;297:R1283-1292.
620 29. Bailey DM. Oxygen and brain death; back from the brink. *Experimental physiology*.
621 2019;104:1769-1779.
622 30. Bailey DM, Young IS, McEneny J, Lawrenson L, Kim J, Barden J and Richardson RS.
623 Regulation of free radical outflow from an isolated muscle bed in exercising humans.
624 *American Journal of Physiology (Heart and Circulatory Physiology)*. 2004;287:H1689-H1699.

medRxiv preprint doi: https://doi.org/10.1101/2023.07.24.23293124; this version posted July 27, 2023. The copyright holder for this preprint
(which was not certified by peer review) is the author/funder, who has granted medRxiv a license to display the preprint in perpetuity.
It is made available under a CC-BY-NC-ND 4.0 International license .

31. Janigro D, Bailey DM, Lehmann S, Badaut J, O'Flynn R, Hirtz C and Marchi N. Peripheral blood and salivary biomarkers of blood–brain barrier permeability and neuronal damage: clinical and applied concepts. *Frontiers in Neurology*. 2021.

32. Jia L, Bonaventura C, Bonaventura J and Stamler JS. S-nitrosohaemoglobin: a dynamic activity of blood involved in vascular control. *Nature*. 1996;380:221-6.

33. Cosby K, Partovi KS, Crawford JH, Patel RP, Reiter CD, Martyr S, Yang BK, Waclawiw MA, Zalos G, Xu X, Huang KT, Shields H, Kim-Shapiro DB, Schechter AN, Cannon RO and Gladwin MT. Nitrite reduction to nitric oxide by deoxyhemoglobin vasodilates the human circulation. *Nature Medicine*. 2003;9:1498-505.

34. Dimmeler S, Fleming I, Fisslthaler B, Hermann C, Busse R and Zeiher AM. Activation of nitric oxide synthase in endothelial cells by Akt-dependent phosphorylation. *Nature*. 1999;399:601-5.

35. O'Gallagher K, Rosentreter RE, Elaine Soriano J, Roomi A, Saleem S, Lam T, Roy R, Gordon GR, Raj SR, Chowienczyk PJ, Shah AM and Phillips AA. The Effect of a Neuronal Nitric Oxide Synthase Inhibitor on Neurovascular Regulation in Humans. *Circ Res*. 2022;131:952-961.

36. Gladwin MT, Shelhamer JH, Schechter AN, Pease-Fye ME, Waclawiw MA, Panza JA, Ognibene FP and Cannon RO, III. Role of circulating nitrite and S-nitrosohemoglobin in the regulation of regional blood flow in humans. *Proceedings of the National Academy of Sciences of the United States of America*. 2000;97:11482-11487.

37. Stamler J, Jia L, Eu J, McMahon T, Demchenko I, Bonaventura J, Gernet K and Piantadosi C. Blood Flow Regulation by *S*-Nitrosohemoglobin in the Physiological Oxygen Gradient. *Science*. 1997;276:2034-2037.

medRxiv preprint doi: https://doi.org/10.1101/2023.07.24.23293124; this version posted July 27, 2023. The copyright holder for this preprint (which was not certified by peer review) is the author/funder, who has granted medRxiv a license to display the preprint in perpetuity. It is made available under a CC-BY-NC-ND 4.0 International license .

38. Pawloski JR, Hess DT and Stamler JS. Export by red blood cells of nitric oxide bioactivity. *Nature*. 2001;409:622-6.

39. Ladurner A, Schmitt CA, Schachner D, Atanasov AG, Werner ER, Dirsch VM and Heiss EH. Ascorbate stimulates endothelial nitric oxide synthase enzyme activity by rapid modulation of its phosphorylation status. *Free radical biology & medicine*. 2012;52:2082-90.

40. McMahon TJ, Moon RE, Luschinger BP, Carraway MS, Stone AE, Stolp BW, Gow AJ, Pawloski JR, Watke P, Singel DJ, Piantadosi CA and Stamler JS. Nitric oxide in the human respiratory cycle. *Nature Medicine*. 2002;8:711-7.

41. Gladwin MT, Wang X, Reiter CD, Yang BK, Vivas EX, Bonaventura C and Schechter AN. S-Nitrosohemoglobin is unstable in the reductive erythrocyte environment and lacks O2/NO-linked allosteric function. *The Journal of biological chemistry*. 2002;277:27818-28.

42. Wang X, Bryan NS, MacArthur PH, Rodriguez J, Gladwin MT and Feelisch M. Measurement of nitric oxide levels in the red cell: validation of tri-iodide-based chemiluminescence with acid-sulfanilamide pretreatment. *The Journal of biological chemistry*. 2006;281:26994-7002.

43. Huang Z, Shiva S, Kim-Shapiro DB, Patel RP, Ringwood LA, Irby CE, Huang KT, Ho C, Hogg N, Schechter AN and Gladwin MT. Enzymatic function of hemoglobin as a nitrite reductase that produces NO under allosteric control. *Journal of Clinical Investigation*. 2005;115:2099-107.

44. Guzy R, Hoyos B, Robin E, Chen H, Liu L, Mansfield K, Simon M, Hammerling U and Schumacker P. Mitochondrial complex III is required for hypoxia-induced ROS production and cellular oxygen sensing. *Cell Metabolism*. 2005;1:401-8.

45. Williams NH and Yandell JK. Outer-sphere electron-transfer reactions of ascorbic anions. *Australian Journal of Chemistry*. 1982;35:1133-1144.

medRxiv preprint doi: https://doi.org/10.1101/2023.07.24.23293124; this version posted July 27, 2023. The copyright holder for this preprint (which was not certified by peer review) is the author/funder, who has granted medRxiv a license to display the preprint in perpetuity. It is made available under a CC-BY-NC-ND 4.0 International license .

672 46. Buettner GR. The pecking order of free radicals and antioxidants: lipid peroxidation, a-
673 tocopherol, and ascorbate. *Archives of Biochemistry and Biophysics*. 1993;300:535-543.

674

675 LEGENDS

676 **Figure 1. Experimental hypotheses (A) and design (B)**

677 A. Predicted differential disruption of cerebral redox homeostasis and implications for
678 cerebral bioenergetic function in response to pathological extremes of oxygen (O_2) and
679 carbon dioxide (CO_2) during hypoxemic hypercapnia (HHA, prior normoxic normoventilation)
680 and isolated hyperoxemic hypercapnia (IHA, prior hyperoxic hyperventilation) apneas. O_2/CO_2
681 sensing by the red blood cell (RBC) and mitochondrion is allosterically coupled to formation
682 of nitric oxide ($NO^{\bullet}$)[43] and reactive oxygen/nitrogen (ROS/RNS)[44] species that titrate (global)
683 cerebral blood flow (gCBF) coupling substrate (O_2 and glucose) delivery to demand. The more
684 marked reduction in arterial partial pressure of oxygen (PO_2) during the HHA trial is
685 hypothesized to induce a more pronounced elevation in cerebral oxidative-nitrosative stress
686 (OXNOS) reflected by a free radical-mediated reduction in vascular NO bioavailability
687 (manifest as increased net cerebral output of free radicals and lipid peroxidants and
688 corresponding lower net cerebral uptake of nitrite (NO_2^-) or *S*-nitrosohemoglobin (SNO-Hb)
689 leading to a suppression of cerebral hypoxic vasodilation relative to IHA trial. Note typical
690 human experimental setup highlighting arterial-jugular venous (transcerebral) sampling of
691 blood combined with volumetric assessment of gCBF. $R^{\bullet}$, free radical; NO_2^-, nitrite; N_2O_3,
692 nitrogen tri-oxide; $ONOO^-$, peroxynitrite (not measured); PaO_2, arterial partial pressure of
693 oxygen; $PaCO_2$, arterial partial pressure of carbon dioxide; a-jv_D, arterio-jugular venous
694 concentration difference; SNA, sympathetic nervous activity (not measured). B. Two

medRxiv preprint doi: https://doi.org/10.1101/2023.07.24.23293124; this version posted July 27, 2023. The copyright holder for this preprint
(which was not certified by peer review) is the author/funder, who has granted medRxiv a license to display the preprint in perpetuity.
It is made available under a CC-BY-NC-ND 4.0 International license .

submaximal (practice) apneas preceded separate trials involving prior normoxic (21 % O_2) normoventilation resulting in severe hypoxemic hypercapnia apnea (HHA) whereas the second followed prior hyperoxic hyperventilation (100 % O_2), designed to prevent hypoxemia resulting in isolated hypercapnic apnea (IHA). The first practice apnea was performed at functional residual capacity (FRC) for 6 involuntary body movements (IBMs) and the second practice at total lung capacity (TLC) for 10 IBMs. Both maximal apneas were performed at TLC. Measurements were performed at baseline and timed to coincide with the end of each maximal apnea.

Figure 2. Transcerebral exchange of oxidative stress biomarkers

Values are mean ± SD; Separate trials involving prior normoxic (21 % O_2) normoventilation resulting in severe hypoxemic hypercapnia apnea (HHA) whereas the second followed prior hyperoxic (100 % O_2) hyperventilation, designed to prevent hypoxemia resulting in isolated hypercapnic apnea (IHA); Circles and triangles denote individual data points for participants during the NX and HX trials respectively; Total lipid soluble antioxidants (LSA) calculated as the cumulative concentration of α/γ-tocopherol, α/β-carotene, retinol and lycopene; $A^{\cdot-}$, ascorbate free radical; LOOH, lipid hydroperoxides. Exchange calculated as the product of global cerebral plasma/serum flow and arterio-jugular venous concentration difference. Positive or negative gradients reflect net cerebral uptake (loss or consumption) or output (gain or formation) respectively. Since the concentration of ascorbate in human plasma is orders of magnitude greater than any oxidizing free radical combined with the low one-electron reduction potential for the $A^{\bullet-}$/ascorbate monanion (AH^-) couple ($E^{\circ\prime}$ = 282 mV)[45], any oxidizing species ($R^{\bullet}$) generated locally within the cerebral circulation will result in the one-electron oxidation of ascorbate to form the distinctive EPR-detectable $A^{\bullet-}$ doublet ($R^{\bullet}$ +

medRxiv preprint doi: https://doi.org/10.1101/2023.07.24.23293124; this version posted July 27, 2023. The copyright holder for this preprint (which was not certified by peer review) is the author/funder, who has granted medRxiv a license to display the preprint in perpetuity. It is made available under a CC-BY-NC-ND 4.0 International license .

719 $AH^- \rightarrow A^{\bullet -}$ + R-H, Panel D inset with main coupling hydrogen highlighted in red)[46]. *different

720 between state for given trial ($P < 0.05$); †different between trial for given state ($P < 0.05$).

721

722

723

724 **Figure 3. Local distribution of nitric oxide (NO) metabolites**

725 Values are mean ± SD; Separate trials involving prior normoxic (21 % O_2) normoventilation

726 resulting in severe hypoxemic hypercapnia apnea (HHA) whereas the second followed prior

727 hyperoxic hyperventilation (100 % O_2), designed to prevent hypoxemia resulting in isolated

728 hypercapnic apnea (IHA); NO, nitric oxide; NO_2^-, nitrite; RSNO, *S*-nitrosothiols; SNO-Hb, *S*-

729 nitrosohemoglobin; HbNO, nitrosylhemoglobin; A, arterial; V, venous. Plasma NO_2^-: *Trial (P =*

730 *0.010); State (P = 0.003); Site (P = <0.001); Trial × Site (P = 0.048);* RBC NO_2^-: *Trial (P = 0.048);*

731 *Site (P = 0.047);* SNO-Hb: *Trial (P = 0.014); State (P = 0.036); Site (P = 0.019); Trial × State (P =*

732 *0.022);* HbNO: *Trial (P = 0.002); Site (P = <0.001); Trial × State (P = 0.024); Trial × State × Site*

733 *(P = 0.045);* Total plasma NO: *Trial (P = 0.009); State (P = 0.033); Site (P = <0.001); Trial × Site*

734 *(P = 0.042);* Total RBC NO: *State (P = 0.042);* Total plasma + RBC NO: *Trial (P = 0.044); Site (P =*

735 *0.036).* *different between state for given trial ($P < 0.05$); †different between trial for given

736 state ($P < 0.05$).

737

738 **Figure 4. Transcerebral exchange of nitrosative stress biomarkers**

739 Values are mean ± SD; Separate trials involving prior normoxic (21 % O_2) normoventilation

740 resulting in severe hypoxemic hypercapnia apnea (HHA) whereas the second followed prior

741 hyperoxic hyperventilation (100 % O_2), designed to prevent hypoxemia resulting in isolated

medRxiv preprint doi: https://doi.org/10.1101/2023.07.24.23293124; this version posted July 27, 2023. The copyright holder for this preprint
(which was not certified by peer review) is the author/funder, who has granted medRxiv a license to display the preprint in perpetuity.
It is made available under a CC-BY-NC-ND 4.0 International license .

hypercapnic apnea (IHA); Circles and triangles denote individual data points for participants during the NX and HX trials respectively; NO, nitric oxide; NO_2^-, nitrite; RSNO, *S*-nitrosothiols; SNO-Hb, *S*-nitrosohemoglobin; HbNO, nitrosylhemoglobin. Exchange calculated as the product of global cerebral plasma (A-C) or red blood cell (RBC, D-G) or whole blood (H) flow and arterio-jugular venous concentration difference. Positive or negative gradients reflect net cerebral uptake (loss or consumption) or output (gain or formation) respectively. Note typical smoothed traces for arterial concentration of metabolites obtained by ozone-based chemiluminescence (same scale). *different between state for given trial ($P < 0.05$); †different between trial for given state ($P < 0.05$).

medRxiv preprint doi: https://doi.org/10.1101/2023.07.24.23293124; this version posted July 27, 2023. The copyright holder for this preprint (which was not certified by peer review) is the author/funder, who has granted medRxiv a license to display the preprint in perpetuity. It is made available under a CC-BY-NC-ND 4.0 International license .

SUPPLEMENTAL MATERIAL

Supplemental Table 1. Blood gas variables

Values are mean ± SD; PO_2/PCO_2, partial pressure of oxygen/carbon dioxide; SO_2, oxyhemoglobin saturation; cO_2, oxygen content; H^+, hydrogen ions HCO_3^-, bicarbonate ions; Hb, hemoglobin; Hct, hematocrit. *different between state for given trial and site ($P < 0.05$); †different between trial for given state and site ($P < 0.05$).

Supplemental Table 2. Cardiopulmonary function

Values are mean ± SD; HR, heart rate; SV, stroke volume; $\dot{Q}$, cardiac output; MAP, mean arterial pressure; IJVP, internal jugular venous pressure; CPP, cerebral perfusion pressure. Δ, apnea minus eupnea; *different between state for given trial ($P < 0.05$); †different between trial for given state or Δ ($P < 0.05$).

Supplemental Table 3. Cerebral bioenergetic function

Values are mean ± SD; $\dot{Q}_{ICA}$, internal carotid artery flow; $\dot{Q}_{VA}$, vertebral artery flow; gCBF, global cerebral blood flow; $gCDO_2$, global cerebral delivery of oxygen; $gCD_{Glucose}$, global cerebral delivery of glucose; CMR, cerebral metabolic rate; Δ, apnea minus eupnea. *different between state for given trial ($P < 0.05$); †different between trial for given state ($P < 0.05$).

Table 1. Oxidative stress

Values are mean ± SD; a-v_D, arterio-jugular venous concentration difference; Total lipid soluble antioxidants (LSA) calculated as the cumulative concentration of α/γ-tocopherol, α/β-carotene, retinol and lycopene; $A^{\cdot-}$, ascorbate free radical; LOOH, lipid hydroperoxides.

medRxiv preprint doi: https://doi.org/10.1101/2023.07.24.23293124; this version posted July 27, 2023. The copyright holder for this preprint
(which was not certified by peer review) is the author/funder, who has granted medRxiv a license to display the preprint in perpetuity.
It is made available under a CC-BY-NC-ND 4.0 International license .

775 Positive or negative a-v_D reflects cerebral uptake (loss or consumption) or output (gain or
776 formation) respectively.

777

778 Table 2. Nitrosative stress

779 Values are mean ± SD; a-v_D, ; NO, nitric oxide; NO_2^-, nitrite; RSNO, *S*-nitrosothiols; SNO-Hb, *S*-
780 nitrosohemoglobin; HbNO, nitrosylhemoglobin. Positive or negative a-v_D reflects cerebral
781 uptake (loss or consumption) or output (gain or formation) respectively. *different between
782 site for given trial and state ($P < 0.05$); †different between trial for given state and site ($P <$
783 0.05).

medRxiv preprint doi: https://doi.org/10.1101/2023.07.24.23293124; this version posted July 27, 2023. The copyright holder for this preprint
(which was not certified by peer review) is the author/funder, who has granted medRxiv a license to display the preprint in perpetuity.
It is made available under a CC-BY-NC-ND 4.0 International license .

ACKNOWLEDGMENTS

The authors acknowledge the cheerful cooperation of all participants. We are also indebted to Professor IS Young and Dr Jane McEneny for specialist technical input.

SOURCES OF FUNDING

This study was funded by a Royal Society Wolfson Research Fellowship (#WM170007) and Higher Education Funding Council for Wales (Dr Bailey), Canada Research Chair (CRC) and Natural Sciences and Engineering Research Council of Canada (NSERC) Discovery grant (Dr Ainslie), NSERC (Drs Bain and Hoiland), Autonomic Province of Vojvodina, Serbia (#142-451-2541, Dr Barak) and Croatian Science Foundation Grant (#IP-2014-09-1937, Drs Barak, Drvis and Ainslie).

DISCLOSURES

Dr Bailey is Editor-in-Chief of Experimental Physiology, Chair of the Life Sciences Working Group, member of the Human Spaceflight and Exploration Science Advisory Committee to the European Space Agency, member of the Space Exploration Advisory Committee to the UK Space Agency, member of the National Cardiovascular Network for Wales and South East Wales Vascular Network and is affiliated to the companies FloTBI, Inc. and Bexorg, Inc. focused on the technological development of novel biomarkers of brain injury in humans.

Supplemental Table 1. Blood gas variables

Trial:	Hypoxemic Hypercapnia Apnea (*n* = 10)				Isolated Hypercapnic Apnea (*n* = 10)			
State:	Eupnea		Apnea		Eupnea		Apnea	
Site:	Arterial	Venous	Arterial	Venous	Arterial	Venous	Arterial	Venous
PO_2 (mmHg)	97 ± 12	34 ± 4	36 ± 5*	28 ± 5*	589 ± 23†	28 ± 10	425 ± 79*†	80 ± 9*†
Trial (P = <0.001); State (P = <0.001); Site (P = <0.001); Trial × Site (P = <0.001); State × Site (P = <0.001); Trial × State × Site (P = <0.001)								
SO_2 (%)	98 ± 1	58 ± 7	60 ± 11*	40 ± 11*	100 ± 0†	51 ± 19	100 ± 0*†	93 ± 2*†
Trial (P = <0.001); Site (P = <0.001); Trial × State (P = <0.001); State × Site (P = <0.001); Trial × State × Site (P = 0.008)								
cO_2 (mL/dL)	18.3 ± 1.7	10.7 ± 1.6	11.7 ± 2.4*	8.0 ± 2.6*	20.6 ± 2.0†	9.7 ± 3.6	20.0 ± 1.6*†	17.8 ± 1.9*†
Trial (P = <0.001); Site (P = <0.001); Trial × State (P = <0.001); State × Site (P = <0.001); Trial × State × Site (P = 0.006)								
PCO_2 (mmHg)	36 ± 5	47 ± 5	51 ± 3*	54 ± 4*	16 ± 4†	31 ± 6†	58 ± 5*†	59 ± 15*
Trial (P = 0.006); State (P = <0.001); Site (P = <0.001); Trial × State (P = <0.001); State × Site (P = <0.001); Trial × State × Site (P = 0.033)								
pH (units)	7.440 ± 0.043	7.384 ± 0.032	7.360 ± 0.023*	7.348 ± 0.021*	7.700 ± 0.078†	7.542 ± 0.071†	7.283 ± 0.043*†	7.306 ± 0.154*
Trial (P = 0.005); State (P = <0.001); Site (P = 0.001); Trial × State (P = <0.001); State × Site (P = <0.001); Trial × State × Site (P = 0.008)								
H^+ (µM)	36 ± 3	41 ± 3	44 ± 2	45 ± 2	20 ± 4	29 ± 4	52 ± 5	52 ± 12
Trial (P = 0.041); State (P = <0.001); Site (P = 0.001); Trial × State (P = <0.001); State × Site (P = <0.001); Trial × State (P = <0.001)								
HCO_3^- (mM)	24.2 ± 2.5	27.9 ± 2.3	27.9 ± 3.1*	29.8 ± 2.0*	19.8 ± 2.0†	26.0 ± 2.2†	27.2 ± 1.9*	27.9 ± 2.1*†
Trial (P = 0.001); State (P = <0.001); Site (P = <0.001); Trial × State (P = 0.002); State × Site (P = <0.001); Trial × State × Site (P = <0.001)								
Hb (g/dL)	13.7 ± 1.4	13.7 ± 1.4	14.3 ± 1.2	14.5 ± 1.0	14.0 ± 1.4	14.2 ± 1.5	14.0 ± 1.2	14.1 ± 1.4
Trial × State (P = 0.034)								
Hct (%)	42 ± 4	42 ± 4	44 ± 4	44 ± 3	43 ± 4	44 ± 5	43 ± 4	43 ± 4
Trial × State (P = 0.023)								

medRxiv preprint doi: https://doi.org/10.1101/2023.07.24.23293124; this version posted July 27, 2023. The copyright holder for this preprint (which was not certified by peer review) is the author/funder, who has granted medRxiv a license to display the preprint in perpetuity. It is made available under a CC-BY-NC-ND 4.0 International license .

Supplemental Table 2. Cardiopulmonary function

Trial:	Hypoxemic Hypercapnia Apnea (*n* = 10)			Isolated Hypercapnic Apnea (*n* = 10)		
State:	Eupnea	Apnea	Δ	Eupnea	Apnea	Δ
HR (b/min)	64 ± 7	59 ± 14	-5 ± 12	65 ± 11	69 ± 13	4 ± 18
SV (mL/min)	78 ± 16	67 ± 16*	-11 ± 15	86 ± 17†	90 ± 17†	5 ± 12†
Trial (P = 0.001); Trial × State (P = 0.001)						
$\dot{Q}$ (L/min)	4.92 ± 0.91	3.91 ± 1.17*	-1.01 ± 1.21	5.46 ± 1.01	6.29 ± 1.97†	0.83 ± 1.73†
Trial (P = 0.001); Trial × State (P = 0.029)						
MAP (mmHg)	116 ± 8	177 ± 8*	61 ± 9	111 ± 8†	158 ± 16*†	47 ± 14*†
Trial (P = 0.001); State (P = <0.001); Trial × State (P = 0.018)						
IJVP (mmHg)	10 ± 2	22 ± 1*	12 ± 2	10 ± 2	17 ± 5*†	7 ± 5*†
Trial (P = 0.015); State (P = <0.001); Trial × State (P = 0.016)						
CPP (mmHg)	106 ± 9	155 ± 7	49 ± 8	101 ± 9	141 ± 16	40 ± 13
Trial (P = 0.002); State (P = <0.001); Trial × State (P = 0.112)						

Supplemental Table 3. Cerebral bioenergetic function

Trial:	Hypoxemic Hypercapnia Apnea (*n* = 10)			Isolated Hypercapnic Apnea (*n* = 10)		
State:	Eupnea	Apnea	Δ	Eupnea	Apnea	Δ
Perfusion						
$\dot{Q}_{ICA}$ (mL/min)	458 ± 55	848 ± 148*	390 ± 119	317 ± 92†	938 ± 211*	621 ± 174†
State (P = <0.001); Trial × State (P = 0.001)						
$\dot{Q}_{VA}$ (mL/min)	177 ± 82	307 ± 133*	130 ± 54	113 ± 55†	357 ± 198*	244 ± 146†
State (P = <0.001); Trial × State (P = 0.009)						
gCBF (mL/min)	635 ± 84	1155 ± 147*	520 ± 114	31 ± 7†	92 ± 22*	865 ± 260†
State (P = <0.001); Trial × State (P = 0.002)						
Metabolism						
$gCDO_2$ (mL/min)	116 ± 22	137 ± 43*	20 ± 30	88 ± 20†	259 ± 63*†	171 ± 52†
Trial (P = <0.001); State (P = <0.001); Trial × State (P = <0.001)						
gCD_{Gluc} (mM/min)	3.45 ± 0.60	6.30 ±1.07*	2.85 ± 0.77	2.20 ± 0.49†	7.48 ± 1.57*†	5.28 ± 1.40†
State (P = <0.001); Trial × State (P = <0.001)						
$gCMRO_2$ (mL/min)	47 ± 8	43 ± 12	-5 ± 17	48 ± 19	28 ± 8	-19 ± 18
State (P = 0.015)						
$gCMR_{Glucose}$ (mM/min)	0.37 ± 0.09	0.30 ± 0.09	-0.07 ± 0.14	0.47 ± 0.14	0.50 ± 0.52	0.04 ± 0.58
Trial (P = 0.044)						

Table 1. Oxidative stress

Trial:	Hypoxemic Hypercapnia Apnea (*n* = 10)				Isolated Hypercapnic Apnea (*n* = 10)			
State:	Eupnea		Apnea		Eupnea		Apnea	
Site:	Arterial	Venous	Arterial	Venous	Arterial	Venous	Arterial	Venous
Antioxidants								
Ascorbate (μM)	59.3 ± 11.0	59.2 ± 10.0	61.8 ± 8.9	53.5 ± 6.4	61.0 ± 6.7	60.5 ± 5.3	63.0 ± 5.6	60.0 ± 3.7
Site (P = 0.007); Trial × Site (P = 0.017); State × Site (P = 0.015)								
a-v_D (μM)	0.2 ± 4.3		8.3 ± 5.6		0.5 ± 4.9		3.0 ± 4.0	
Trial (P = 0.017); State (P = 0.015)								
α-tocopherol (μM)	22.1 ± 3.9	21.7 ± 3.2	24.4 ± 3.0	20.4 ± 3.4	22.5 ± 4.9	22.7 ± 4.1	22.7 ± 2.9	21.3 ± 3.2
Site (P = 0.008); State × Site (P = 0.011)								
a-v_D (μM)	0.3 ± 1.5		4.0 ± 2.6		-0.1 ± 4.2		1.4 ± 2.6	
State (P = 0.010)								
Total LSA (μM)	25.6 ± 3.6	25.2 ± 3.1	28.0 ± 2.6	23.7 ± 3.0	26.0 ± 4.7	26.2 ± 3.9	26.0 ± 2.5	24.4 ± 2.7
Site (P = 0.006); State × Site (P = 0.010)								
a-v_D (μM)	0.4 ± 2.1		4.3 ± 2.4		-0.1 ± 4.7		1.6 ± 2.6	
State (P = 0.011)								
Free radicals								
$A^{\cdot-}$ (AU × 10^2)	320 ± 107	313 ± 98	344 ± 95	473 ± 127	322 ± 70	333 ± 102	363 ± 143	386 ± 129
State (P = 0.009); Site (P = 0.046); State × Site (P = 0.048)								
a-v_D (AU × 10^2)	6 ± 130		-129 ± 96		-12 ± 143		-24 ± 91	
State (P = 0.048)								
Lipid peroxidation								
LOOH (μM)	1.15 ± 0.17	1.16 ± 0.13	1.22 ± 0.25	1.74 ± 1.20	1.19 ± 0.15	1.25 ± 0.22	1.27 ± 0.18	1.45 ± 0.24
State (P = 0.038); Site (P = 0.045); State × Site (P = 0.048)								
a-v_D (μM)	-0.01± 0.14		-0.52 ± 0.97		-0.07 ± 0.23		-0.18 ± 0.15	
State (P = 0.047)								

Table 2. Nitrosative stress

Trial:	Hypoxemic Hypercapnia Apnea (*n* = 10)				Isolated Hypercapnic Apnea (*n* = 10)			
State:	Eupnea		Apnea		Eupnea		Apnea	
Site:	Arterial	Venous	Arterial	Venous	Arterial	Venous	Arterial	Venous
Plasma								
NO_2^- (nM)	161 ± 45	149 ± 35	124 ± 45	85 ± 34	210 ± 80	154 ± 42	176 ± 55	108 ± 45
Trial (P = 0.010); State (P = 0.003); Site (P = <0.001); Trial × Site (P = 0.048)								
a-v_D (nM)	12 ± 48		39 ± 46		55 ± 55		68 ± 34	
Trial (P = 0.048)								
RSNO (nM)	9 ± 9	7 ± 8	8 ± 11	6 ± 9	6 ± 5	4 ± 4	5 ± 6	5 ± 2
a-v_D (nM)	2 ± 6		2 ± 4		1 ± 3		1 ± 4	
Total NO (nM)	170 ± 43	155 ± 37	132 ± 52	91 ± 39	215 ± 82	159 ± 45	181 ± 58	113 ± 47
Trial (P = 0.009); State (P = 0.033); Site (P = <0.001); Trial × Site (P = 0.042)								
a-v_D (nM)	14 ± 46		41 ± 46		57 ± 55		68 ± 37	
Trial (P = 0.042)								
Red blood cell								
NO_2^- (nM)	171 ± 62	138 ± 39	190 ± 71	158 ± 52	216 ± 84	174 ± 65	202 ± 72	210 ± 96
Trial (P = 0.048); Site (P = 0.047)								
a-v_D (nM)	33 ± 64		33 ± 94		42 ± 106		-8 ± 128	
SNO-Hb (nM)	10 ± 3	15 ± 5	16 ± 5	32 ± 30	9 ± 4	14 ± 6	9 ± 3	12 ± 3
Trial (P = 0.014); State (P = 0.036); Site (P = 0.019); Trial × State (P = 0.022)								
a-v_D (nM)	-5 ± 5		-16 ± 31		-5 ± 6		-3 ± 5	
HbNO (nM)	21 ± 5	41 ± 15*	32 ± 20	66 ± 38*	7 ± 3†	30 ± 16*	11 ± 8†	24 ± 17†
Trial (P = 0.002); Site (P = <0.001); Trial × State (P = 0.024); Trial × State × Site (P = 0.045)								
a-v_D (nM)	-20 ± 16		-34 ± 31		-1 ± 13		-29 ± 33†	
Trial × State (P = 0.049)								
Total NO (nM)	202 ± 62	194 ± 47	239 ± 81	256 ± 81	232 ± 81	218 ± 65	222 ± 72	245 ± 103
State (P = 0.042)								
a-v_D (nM)	8 ± 68		-17 ± 120		14 ± 112		-24 ± 139	
Plasma + Red blood cell								
Total NO (nM)	371 ± 69	349 ± 50	371 ± 103	347 ± 107	447 ± 96	376 ± 93	403 ± 88	358 ± 134
Trial (P = 0.044); Site (P = 0.036)								
a-v_D (nM)	22 ± 68		24 ± 140		71 ± 85		44 ± 161	

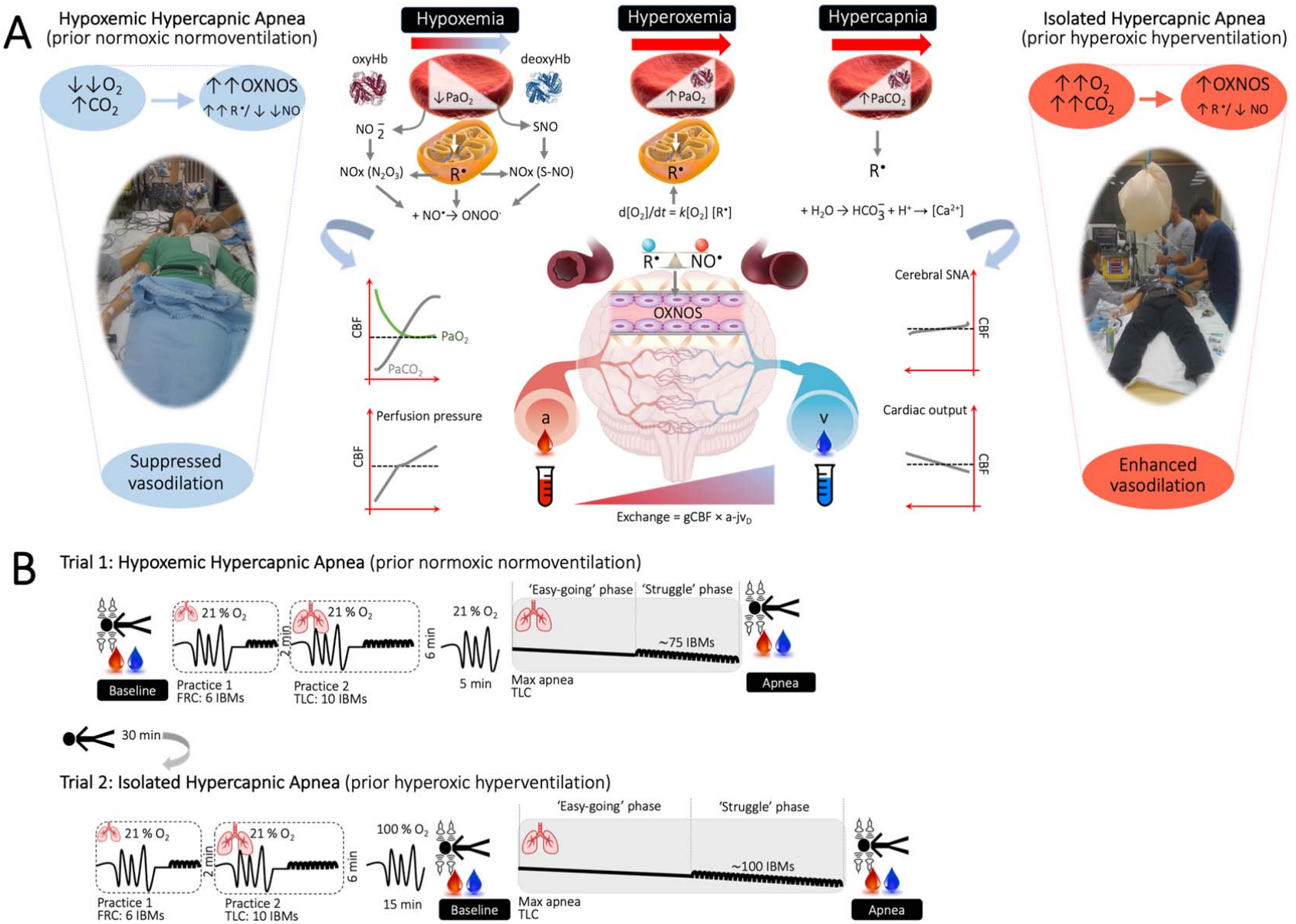

Figure 1. Experimental hypotheses (A) and design (B)

medRxiv preprint doi: https://doi.org/10.1101/2023.07.24.23293124; this version posted July 27, 2023. The copyright holder for this preprint
(which was not certified by peer review) is the author/funder, who has granted medRxiv a license to display the preprint in perpetuity.
It is made available under a CC-BY-NC-ND 4.0 International license .

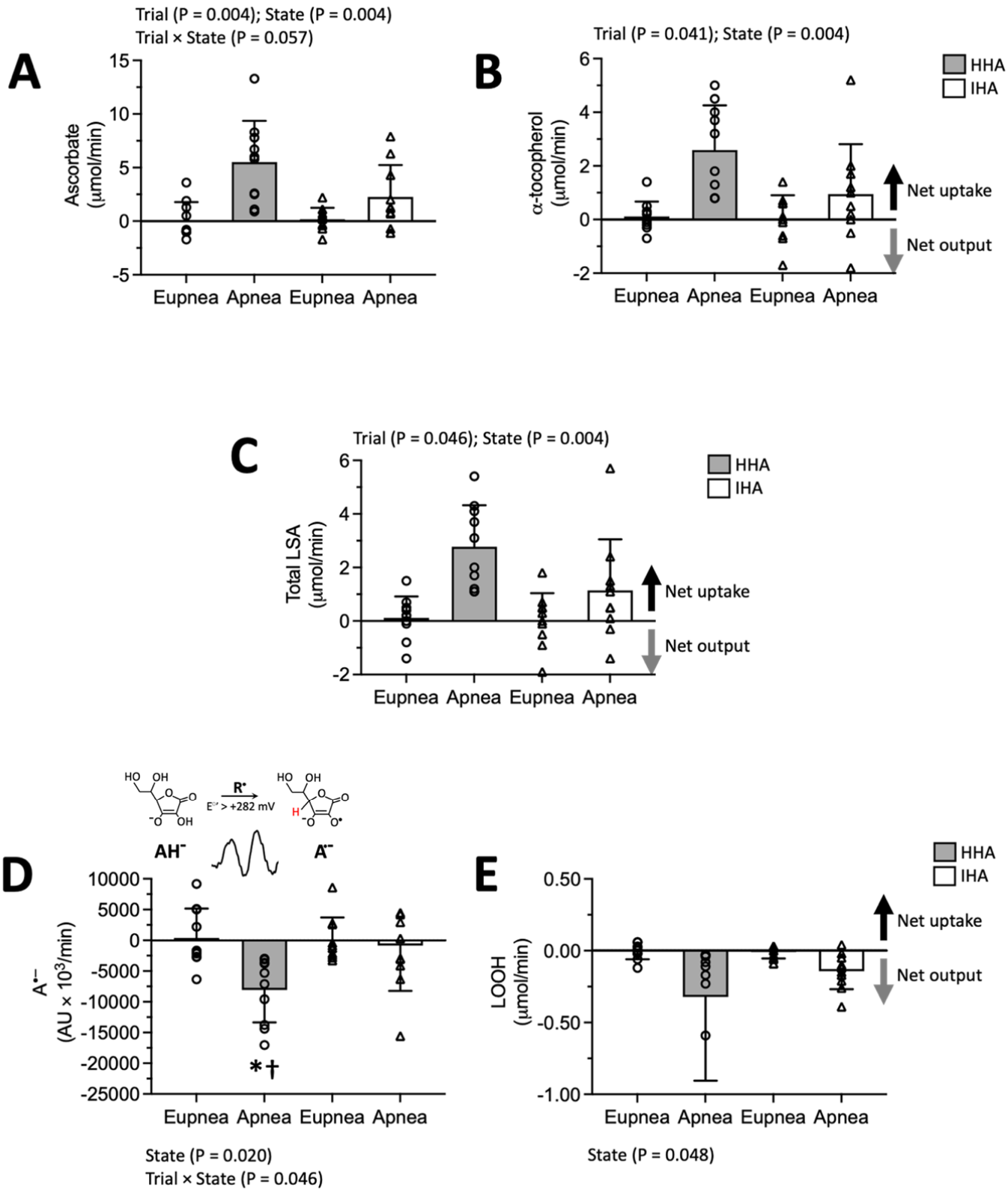

Figure 2. Transcerebral exchange of oxidative stress biomarkers

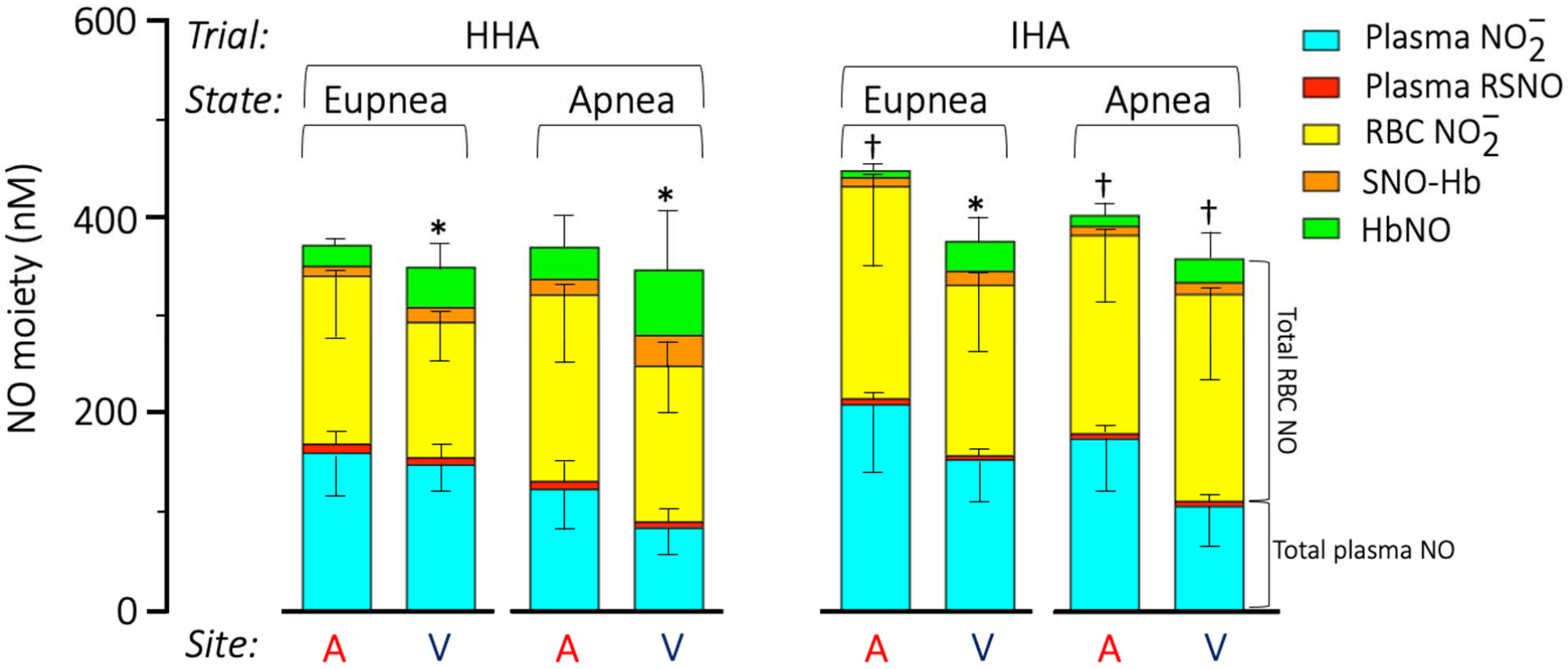

Figure 3. Local distribution of nitric oxide (NO) metabolites

medRxiv preprint doi: https://doi.org/10.1101/2023.07.24.23293124; this version posted July 27, 2023. The copyright holder for this preprint
(which was not certified by peer review) is the author/funder, who has granted medRxiv a license to display the preprint in perpetuity.
It is made available under a CC-BY-NC-ND 4.0 International license .

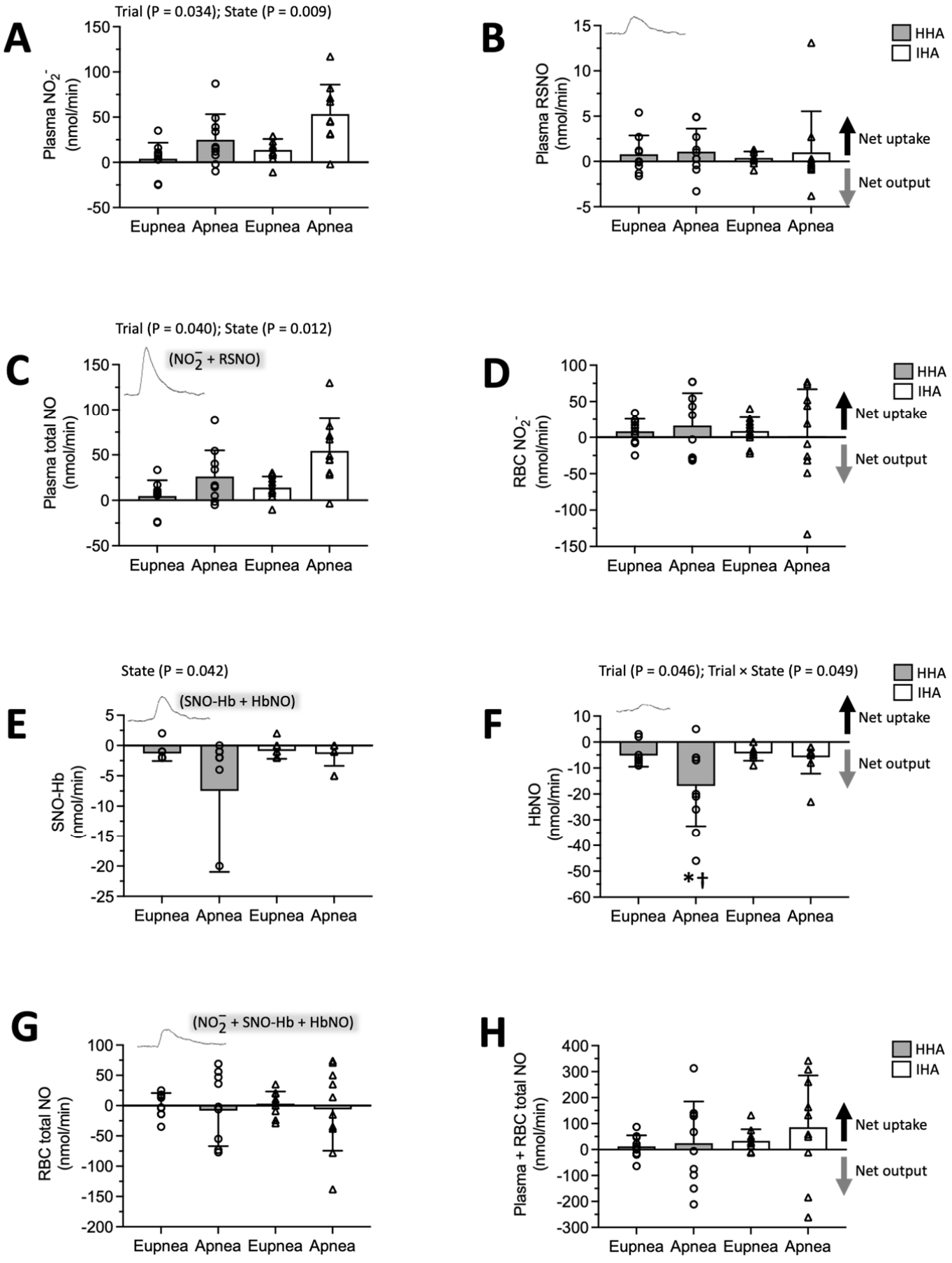

Figure 4. Transcerebral exchange of nitrosative stress biomarkers